

Design, Molecular Docking And In Silico Analysis Of Analogues Of Chloroquine And Hydroxychloroquine Against SARs-COV-2 Target (6w63.pdb)

Naruka Solomon Yakubu (✉ yakubun@unijos.edu.ng)

University of Jos <https://orcid.org/0000-0001-9066-8757>

Olanike Catherine Poyi

University of Jos

Ezekiel Olabisi Afolabi

University of Jos

Research Article

Keywords: COVID-19, SARS-CoV-2, Docking, Chloroquine, Hydroxychloroquine

Posted Date: July 8th, 2020

DOI: <https://doi.org/10.21203/rs.3.rs-40615/v1>

License:  This work is licensed under a Creative Commons Attribution 4.0 International License.

[Read Full License](#)

Abstract

Computer-aided drug design has been an effective strategy and approach to discover, develop, analyze, accelerate and economize design and development of drugs and biologically active molecules. A total of twelve analogues of chloroquine (CQ) and hydroxychloroquine (HCQ) were designed and virtually analyzed using PyRx software, Molinspiration, Swiss ADME, Swiss-Target Prediction software and ProTox-II-Prediction of toxicity platform. Based on the docking studies carried out using Autodock vina, five analogues; H-368 (-6.0 Kcal/mol), H-372 (-6.0 Kcal/mol), H-156 (-5.9 Kcal/mol), H-139 (-5.7 Kcal/mol), C-136 (-5.7 Kcal/mol) exhibited higher binding affinity compared to HCQ(-5.5 Kcal/mol), while all twelve analogues exhibited higher binding affinity compared to CQ (-4.5Kcal/mol). In silico analysis of toxicity profile of this analogues shows a lower potential to toxicity and a comparable activity on some major isoforms of cytochrome P450. But unlike the parent molecules, both H-139 and H-156 are substrates of P-glycoproteins (P-gp) which implies that these analogues possess high clearance and less pharmacokinetic-related drug-drug interactions compared to the parent molecules. Herein we propose these analogues as potential inhibitors or lead compounds against the coronavirus with a view of conducting more molecular dynamic simulations, synthesizing and conducting in vitro studies on them.

Introduction

The world is faced with skyrocketing costs for drug design and development of new biologically active molecules hence researchers are currently looking for ways to repurpose older drugs-and possibly, even some that failed in initial trials. With the aid of computer-aided drug-design and development, researchers can find countless new tricks for old drugs [1]. According to Atul Butte (2012), a bioinformatician at the University of California, San Francisco, drug repositioning is a complement to the discovery of new molecules, rather than an alternative. More so, modern medicine is becoming better at figuring out that each disease is actually five or ten different ones and there are simply not enough companies out there to develop new drugs to treat them all [2]. For researchers in the academia and industries, taking drugs that have been developed for one disorder and repositioning them-with little or no modification to tackle another disorder/disease, is an increasingly important strategy for researchers. These efforts are been inspired from numerous classic success stories as documented in many literatures [3]. In the same light, drugs like chloroquine and hydroxychloroquine (Fig. 1) is the focus of our research here.

The serendipity responsible for the earlier discovery of drugs like chloroquine (Fig.1a) for the prevention and treatment of malaria and hydroxychloroquine (Fig. 1b) for the treatment of malaria, rheumatoid arthritis, lupus and porphyria cutanea cannot be overemphasized as they are currently being studied in order to be repositioned for the treatment of COVID-19 [4]. However, according to Mittra and Mieler 2013, these drugs/molecules are not without some serious side effects (seizures, muscle damage, problems with vision, low blood count, etc.) that can possibly limit their potential application in other disease

conditions. Consequently, computational chemistry is being applied to design twelve (12) analogues of (a) and (b) in order to potentiate their safety, efficacy and overall potency against the dreaded COVID–19.

The rapid spread of SARS-CoV–2 Virus (Fig. 2) and the growing number of deaths have catalyzed an unprecedented response by both the medical and scientific communities to tackle the COVID–19 disease- from understanding its epidemiology to resolving its molecular structures, understanding the mechanisms of its druggable protein targets, identifying effective therapeutic agents and developing vaccines to prevent further spread of the virus.

Identifying key protein targets for drug development is one of the first tasks to be addressed. Once a druggable protein model or structure is available, numerous molecular modelling methods allow us to identify drugs with high specificity and efficacy. While these methods involve de novo design strategies, the urgency of the current of situation makes drugs repurposing one of the most economic and efficient therapeutic strategies to pursue. We can also leverage on the vast reservoir of knowledge about agents currently known to be effective against SARS-CoV. Virtual screening methods including docking and pharmacophore modelling are ideal to identify and rank-prioritize lead candidates for further investigation and possible optimization. Worthy of note is the fact that relying on physical experimentation alone is not economically sustainable in today's rapidly evolving COVID–19 environment.

Materials And Methods

Hardware

All the computational analysis/screening were done using x64-based PC, windows 10 Pro, 4 compute cores 2C+2G, 2 CORES, 4 GB memory and 32-Bit operating system.

Protein and Ligand Library

12 analogues of CQ and HCQ were designed in PubChem Sketcher V2.4 [5] and downloaded as an MDL file. The structures were optimized and converted to.sdf in discovery studio 4.5 visualizer [6].

The crystal structure of the SARS- CoV–2 target (6W63.pdb) was downloaded from the protein data bank [7], its original ligands and water were eliminated using discovery studio 4.5 visualizer [6].

Molecular Docking

Ligands and Protein target for molecular docking were prepared in Autodock Tools using PyRx 0.8 package [8](27), a grid box (x: –2. 3200, y: 19. 1496, z: –26. 3281, dimensions (Angstrom); x:y:z: = 25.0000) was employed, and docking simulations of bioactive conformations was done using Autodock Vina [8]. The results obtained were analyzed using PyMol [9] and discovery studio visualizer [6].

***In Silico* Pharmacokinetic Studies**

All the structures were drawn using Swiss ADME platform, the SMILES were generated and loaded onto the molinspiration platform where pharmacokinetic properties, bioactivity scores and other parameters were being obtained.

All the molecules were also loaded into the ProTox-II virtual lab in the form of a 'MOLfile' with the aid of Advanced Chemistry Development, Inc.-ACD/Labs, ACD/ChemSketch software [10]. The organ toxicity (hepatotoxicity), toxicity end point (carcinogenicity, immunotoxicity, mutagenicity, cytotoxicity), LD₅₀ and the toxicity class of all the compounds were determined.

Results And Discussion

Understanding binding affinity is key to appreciation of the intermolecular interactions driving biological processes, structural biology and structure-function relationships. It is also measured as part of the drug discovery process to help design drugs that bind their targets selectively and specifically. Binding affinity is the strength of the binding interaction between a single biomolecule (e.g. protein or DNA) to its ligand/binding partner-drug or inhibitor. Binding affinity is typically measured and reported by the dissociation constant-K_D, the smaller the K_D value, the greater the binding affinity of the ligand for its target. [11]. Binding energy is released when a drug molecule associates with a target leading to a lowering of the overall energy of the complex. The release in binding energy also compensates for any transformation of the ligand from its energy minimum to its bound conformation with the protein [12,13].

With respect to the structure-activity relationship (SAR) of these molecules, as summarized in Table 1, the removal of one ethyl group from the terminal nitrogen atom of CQ increased the binding affinity of the molecule with a characteristic binding energy of - 4.5 Kcal/mol (CQ) to - 4.7 Kcal/mol (C-383). Further hydroxylation of the ethyl group led to a further increase in binding affinity with a corresponding binding energy of - 5.7 Kcal/mol (H-139). This can also be seen in the binding interaction of C-136 (Fig. 3d), where the hydrogens of the terminal amino group participated in hydrogen-bonding. The 3D view of binding conformation of H-372, H-156, and C-136 to the active site residues of SARS-CoV-2-6W63.pdb showing hydrogen-bond interactions is shown in Fig. 4. The complete conversion of the two alkyl groups attached to the terminal nitrogen of HCQ to alcoholic groups also led to an increase in binding affinity with a binding energy of -5.9 Kcal/mol (H-156). Also, the removal of C-11 along with the amino group attached to C-9 and C-10 led to an increase in binding affinity of the molecule H-372 (-6.0 Kcal/mol). All the designed molecules have a synthetic accessibility-SA of less than 3. A compound's SA is a very important aspect of computer-aided drug design since in some cases computer-designed compounds/molecules cannot be synthesized [14]. It is often reported within the range of 1 (very easy to synthesize) and 10 (difficult to synthesize).

Due to technical limitations, Table 1 is provided in the Supplementary Files section.

The LogP values (Table 2) of all the molecules are within the range of 2 and less than 5 which indicate compounds of intermediate polarity, good balance between aqueous and lipid solubility, good absorption and distribution. The logP value of a compound, which is the logarithm of its partition coefficient between n-octanol and water i.e. $\log(C_{\text{octanol}}/C_{\text{water}})$, is a well-established measure of the compound's hydrophilicity. Low hydrophilicity, and therefore high logP values poor absorption or permeation. It has been shown for compounds to have reasonable probability of been well absorbed their logP values must not be greater than 5.0 [15].

The designed molecules possess up to 60% activity on the G-protein-coupled receptors (GPCRs) (Table 2) specifically on the family A (rhodopsin-like receptors) as obtained on the Swiss-Target platform. Presently, there are over four hundred (400) drug molecules i.e. approximately 34% of all FDA approved drugs, that act on more than 100 unique targets of GPCRs. Generally, GPCRs are among the most numerous groups of transmembrane proteins of the mammalian genome. Till date, about 800 of these proteins have been identified in humans [16]. The relevance of their manifold functions has made them therapeutically attractive as shown by the fact that they are the targets of over 30% of united states Food and Drug Administration-approved drugs [17]. Two analogues of HCQ (H-139 and H-156) are substrates of the permeability-glycoprotein (P-gp) which implies that these molecules will undergo less pharmacokinetic-related drug-drug interactions and will also be easily cleared from the human system. The knowledge about compounds being substrate or non-substrate of P-gp is key to appraise active efflux through biological membranes, for instance from the git wall to the lumen or from the brain [18]. One important role of the P-gp is to protect the CNS from xenobiotics [19].

Table2: Pharmacokinetic properties and Toxicity Prediction

S/N	Name	LogP	B.A Score	G.I Absorption	BBB	GPCRs (%)	P-gp	LD50 (mg/Kg)	T.C
1	CQ	4.15	0.55	High	Yes	60.0	No	311	4
2	HCQ	3.37	0.55	High	Yes	53.3	No	1240	4
3	C-136	2.83	0.55	High	Yes	60.0	No	750	4
4	H-139	2.77	0.55	High	Yes	53.3	Yes	1240	4
5	H-156	2.88	0.55	High	Yes	53.3	Yes	1240	4
6	C-189	3.49	0.55	High	Yes	60.0	No	311	4
7	H-140	3.36	0.55	High	Yes	60.0	No	750	4
8	C-383	3.57	0.55	High	Yes	53.3	No	311	4
9	H-7715	3.67	0.55	High	Yes	60.0	No	750	4
10	H-97	3.36	0.55	High	Yes	53.3	No	750	4
11	H-368	3.32	0.55	High	Yes	26.7	No	200	3
12	H-372	4.8	0.55	High	Yes	40.0	No	416	4
13	H-369	2.95	0.55	High	Yes	53.3	No	750	4
14	H-347	3.12	0.55	High	Yes	53.3	No	750	4

The interaction of the molecules with CYP450 isoforms and kinase is as presented in Table 3. The HCQ analogue (H-156) stands out as it inhibits only one isoform of CYP450 i.e. CYP2D6 and as earlier mentioned, H-156 is also a substrate of P-gp. The knowledge about interaction of molecules with CYP450 is essential because it plays a major role in drug elimination through metabolic biotransformation. It's being documented that both CYP and P-gp can synergistically process small molecules to improve the protection of tissues and most therapeutic molecules are substrate of five major isoforms (Table 3). Inhibition of these major isoforms is certainly one major cause of pharmacokinetic-related drug-drug interactions leading to toxic or other unwanted adverse effects due to lower clearance and accumulation of the drug or its metabolite. It is therefore important for drug discovery to predict the propensity with which the molecule will cause significant drug interactions through inhibition of CYPs and to determine which isoforms are affected. [20,21]

Table 3: Enzyme activity

CYP450 Isoforms Inhibitors							
S/N	Name	Kinase Inhibitor	CYP1A2	CYP2C19	CYP2C9	CYP2D6	CYP3A4
1	CQ	0.38	Yes	No	No	Yes	Yes
2	HCQ	0.44	Yes	No	No	Yes	No
3	C-136	0.46	Yes	Yes	No	Yes	Yes
4	H-139	0.46	Yes	No	No	Yes	Yes
5	H-156	0.43	No	No	No	Yes	No
6	C-189	0.41	Yes	No	No	Yes	Yes
7	H-140	0.33	Yes	No	No	Yes	No
8	C-383	0.40	Yes	Yes	No	Yes	Yes
9	H-7715	0.44	Yes	No	No	Yes	Yes
10	H-97	0.52	Yes	No	No	Yes	Yes
11	H-368	0.04	Yes	No	No	Yes	Yes
12	H-372	-0.01	Yes	Yes	No	Yes	Yes
13	H-369	0.55	Yes	No	No	Yes	Yes
14	H-347	0.49	Yes	No	No	Yes	Yes

Conclusion

In this study, twelve analogues of CQ and HCQ were designed and subjected to virtual screening, five lead molecules showed better binding affinity and strong interactions with active site residues of SARS-CoV-2 target (6W63.pdb) while all the analogues exhibited superior binding affinity compared to CQ. They were seen to have a number of non-covalent interactions which included, hydrogen bonding, van der waal's forces and hydrophobic interactions. Based on the predicted synthetic accessibility, the compounds can easily be synthesized and in vitro testing can be carried out against the SARS-CoV-2 Vero cell lines as well as comparative toxicity studies using drosophila model prior to subsequent clinical evaluations.

Declarations

CONFLICT OF INTEREST

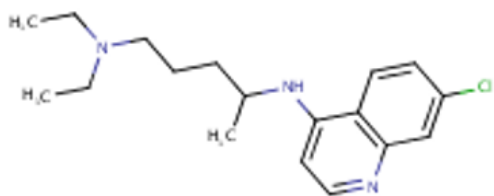
The authors declare that there is no conflict of interest.

References

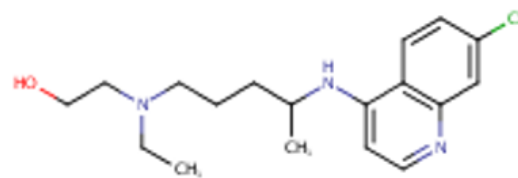
1. Scandl, J. W., Blanckly A., Boldon, H. and Warrington, B. (2012). *Nature Rev. Drug Discov.* 11, 191–200
2. Lekka, E., Deftereos, S. N., Persidis, A. and Andronis, C. (2011). *Drug Discov. Today Ther. Strateg.* 8, 103–108
3. Singh, N., Halliday, A., Thomas, J. et al. (2013). A safe lithium mimetic for bipolar disorder. *Nat Commun* 4, 1332 <http://dx.doi.org/10.1038/ncomms2320>
4. Cortegiani A., Ingoglia G., Ippolito M., Giarratano A., Einav S. (2020). A systematic review on the efficacy and safety of chloroquine for the treatment of COVID–19
5. Ihlenfeldt, Wolf D et al. (2009): “The PubChem chemical structure sketcher.” *Journal of cheminformatics* vol. 1,1–20., doi:10.1186/1758–2946–1–20
6. Dassault Systemes BIOVIA (2016) Discovery Studio Modeling Environment, Release 2017, San Diego.
7. Stephen K Burley, Helen M. Berman, et al. (2019)RCSB Protein Data Bank: biological macromolecular structures enabling research and education in fundamental biology, biomedicine, biotechnology and energy *Nucleic Acids Research* 47: D464–D474. doi: 10.1093/nar/gky1004. <https://www.rcsb.org/>
8. O.Trott., A.J Olson. (2010). Autodock Vina: improving the speed and accuracy of docking with a new scoring function, efficient optimization and multithreading, *journal of computational chemistry* 455–461
9. The PyMOL Molecular Graphics System, Version 1.2r3pre, Schrödinger, LLC
10. ACD/Structure Elucidator, version 2018.1, Advanced Chemistry Development, Inc., Toronto, ON, Canada, www.acdlabs.com, 2019.
11. <https://www.malvernpanalytical.com/en/products/measurements-type/binding-affinity>
12. Baron R., Setny P., Mc Cammon J. A. (2010). “Water in cavity-ligand recognition.” *Journal of the American Chemical Society.* 132 (34):12091–12097.
13. Wienken C. J., Baaske P., Rothbauer U., Braun D., Duhr S. (2010). “Protein-binding assays in biological liquids using microscale thermophoresis.” *Nature Communications.* 1(7):100–101
14. Marco Foscatto, Vidar R. Jensen. (2020). Automated in Silico Design of Homogeneous Catalysts.*ACS Catalysis.* 10(3), 2354–2377.Milan Vorsilak, Daniel Svozil Nonpher. (2017). Computational method for design of hard-to-synthesize structures. *Journal of Cheminformatics.* 9(1)
15. Parker, M. A., Kurasch, D. M., Nichols, D. E. (2008). The role of lipophilicity in determining binding affinity and functional activity for 5-HT_{2A} receptor ligands, *Biorg. Med. Chem.* 16, 4661–4669
16. Fredriksson, R., Lagerstrom, M. C., Lundin, L. G., Schioth H. B. (2003). The G-protein-coupled-receptors in the human genome form five main families. Phylogenetic analysis, paralogon groups, and finger prints. *Mol. Pharmacol.*63(6),1256–1272. doi:10.1124/mol.63.6.1256
17. Hauser, A. S., Attwood, M. M., Rask-Andersen, M., Schioth, H. B., Gloriam, D. E. (2017). Trends in GPCR drug discovery: new agents, targets and indications. *Nat. Rev. Drug Discov.* 16(12), 829–842. doi10.1038/nrd.2017.178

18. Szakacs, G., Váradi, A., Ozvegy-Laczka, C. & Sarkadi, B. (2008). The role of ABC transporters in drug absorption, distribution, metabolism, excretion and toxicity (ADME-Tox). *Drug Discov. Today* 13, 379–393.
19. Huang, S.-M. et al. (2008). New era in drug interaction evaluation: US Food and Drug Administration update on CYP enzymes, transporters, and the guidance process. *J. Clin. Pharmacol.* 48, 662–670
20. Veith, H. et al. (2009). Comprehensive characterization of cytochrome P450 isozyme selectivity across chemical libraries. *Nature Biotechnol.* 27, 1050–1055.
21. Mitra R. A. and Mieler W. F. (2013). “Chapter 89-Drug Toxicity of the Posterior Segment.” *Retina* (fifth ed.). pp.1532–1554
22. Antoine Daina, Olivier Michielin, Vincent Zoete. (2017). SwissADME: a free web tool to evaluate pharmacokinetics, drug-likeness and medicinal friendliness of small molecules. *Scientific Reports.* 7(1).
23. Shoichet, B. K. and Kobilka, B. K. (2012). Structure-based drug screening for G-protein coupled receptors. *Trends Pharmacol.Sci.*33,268–272
24. Niswender, C. M. and Conn, P. J. (2010). Mtebotropic glutamate receptors: physiology, pharmacology and disease. *Annu. Rev. Pharmacol.Toxicol.*50,295–322
25. Tian, S. et al. (2015). The application of in silico drug-likeness predictions in pharmaceutical research. *Adv Drug Deliv Rev* 86, 2–10.
26. Hay, M., Thomas, D. W., Craighead, J. L., Economides, C. & Rosenthal, J. (2014). Clinical development success rates for investigational drugs. *Nature Biotechnol.* 32, 40–51.
27. Dahlin, J. L., Inglese, J. & Walters, M. A. (2015). Mitigating risk in academic preclinical drug discovery. *Nature Rev. Drug Discov.* 14, 279–294.
28. www.SwissADME.ch
29. Mishra, N. K., Agarwal, S. & Raghava, G. P. (2010). Prediction of cytochrome P450 isoform responsible for metabolizing a drug molecule. *BMC Pharmacol.* 10, 8.

Figures



(a)



(b)

Figure 1

Structures of Chloroquine (a) and Hydroxychloroquine (b) (source from www.SwissADME.ch)

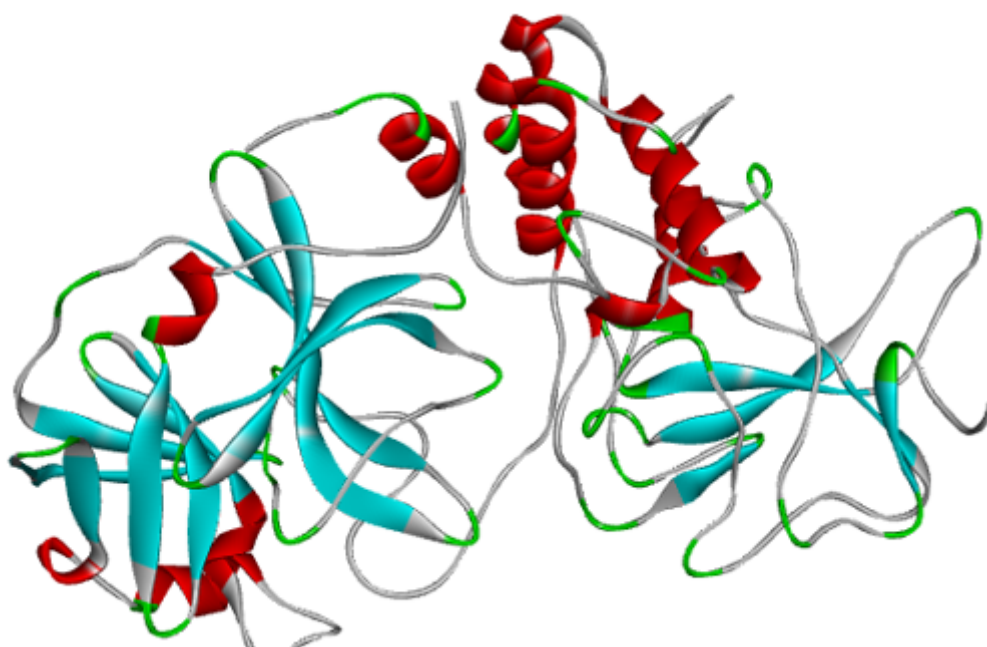


Figure 2

Crystal Structure of SARS-CoV-2 Protein (6W63.pdb)

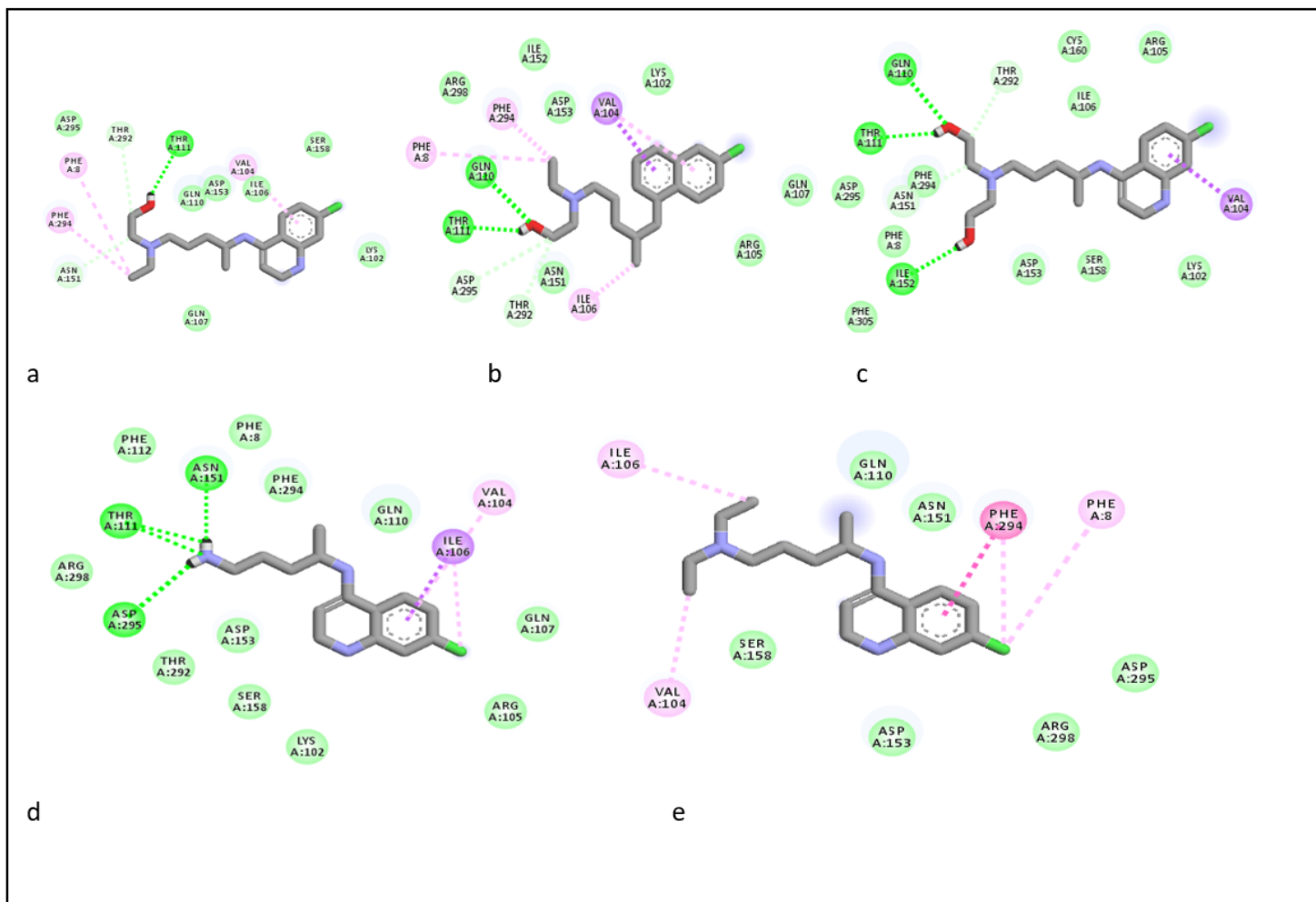


Figure 3

2D binding interactions of HCQ (a), H-372 (b), H-156 (c), C-136 (d) and CQ (e) to the active site residues of SARS-CoV-2 (6W63.pdb). Ligands are shown in stick forms while amino acid residues are shown in disc forms. Hydrogen-bond interaction with amino acid main chain are indicated by green discontinuous lines, green colored discs shows van der waal's interaction while purple discs shows pi-sigma interactions.

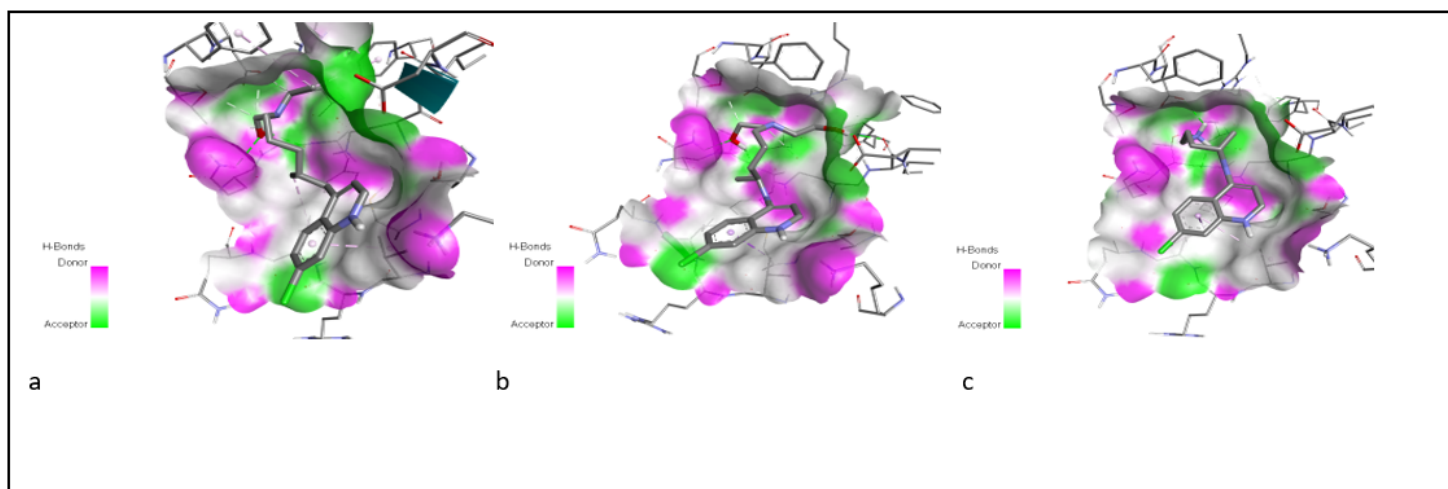


Figure 4

3D view of binding conformation of H-372 (a), H-156 (b), and C-136 (c) to the active site residues of SARS-CoV-2 (6W63.pdb) showing Hydrogen bond interactions.

Supplementary Files

This is a list of supplementary files associated with this preprint. Click to download.

- [Table1.docx](#)